Shotcrete: Elements of a System – Bernard (ed)
© 2010 Taylor & Francis Group, London, ISBN 978-0-415-47589-1

Precision of the ASTM C1550 panel test and field variation in measured FRS performance

E.S. Bernard & G.G. Xu
TSE P/L, Penrith, Australia

N.J. Carino
Consultant, Chagrin Falls, Ohio, USA

ABSTRACT: The ASTM C1550 round panel test has now been used for Quality Control (QC) testing of Fibre Reinforced Shotcrete (FRS) for over 10 years. During that period a large number of specimens have been produced and tested and cumulatively represent a sizeable body of post-crack performance data with which to assess the statistics of FRS performance testing in the filed. Inter-Laboratory Studies (ILS) have also been undertaken to determine the precision of the test method. The present paper describes two recent inter-laboratory studies to establish the single-operator and multi-laboratory precision of ASTM C1550. The studies indicated that coefficient of variation is an appropriate measure of the variability of test results. In general, the two studies resulted in similar indices of precision. In addition, numerous field data have been analyzed to investigate the underlying distribution of individual test results and the variation of test results among replicate test specimens.

1 INTRODUCTION

The ASTM C1550 round panel test, shown in Figure 1 (ASTM, 2008) was first developed in the late 1990s as an alternative to the EFNARC panel test (Roux et al., 1989; EFNARC, 1996), which is now known as the EN 14488 Part 5 square panel test (EN, 2006). Several aspects of fibre reinforced shotcrete (FRS) performance as revealed using the ASTM C1550 test method were first published by Bernard (2000). Later work compared the repeatability of test data using this method with that obtained using beams and EFNARC panels (Bernard, 2002). Additional studies have since examined other aspects of the use of round panels for quality control (QC) assessment in the field (Hanke et al. 2002) and possible sources of error in this test method (Bernard & Pircher, 2001; Bernard, 2005; Bernard & Xu, 2008). As a result, the ASTM C1550 round panel test is a relatively well understood test method and results obtained using this test are specified in guides on the use of shotcrete (ACI, 2008; CIA, 2008).

The ASTM C1550 test offers many advantages over alternative methods of performance assessment, including lower production and testing costs and superior within-batch repeatability. It is now used as part of QC programmes for most projects employing shotcrete in Australia, with the result that approximately 5000 specimens are produced and tested annually. The fact that many of these specimens have been tested using the same servo-controlled testing machine at TSE P/L in Sydney has made it possible to accumulate a large body of data concerning within-batch variability in measured FRS performance for specimens produced in the field. These data have been analysed below to identify characteristic levels of variability and information about the distribution of within-batch results so that the test method can be used rationally and for maximum benefit in future projects.

The present study examines two related topics: the results of a pair of inter-laboratory studies

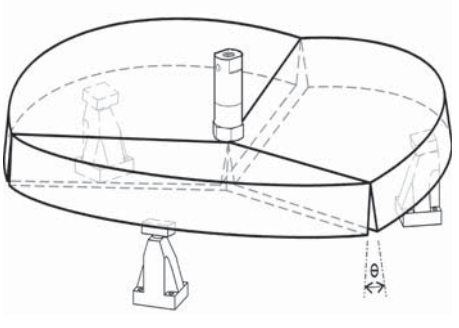

Figure 1. ASTM C1550 round panel test.

(ILS) involving laboratories in Australia, USA, England, and Sweden; and the characteristic distribution of within-batch variability for pairs of specimens produced as part of field QC programmes in Australia.

2 INTER-LABORATORY STUDIES

2.1 *Descriptions of studies*

The first inter-laboratory study (ILS) involved the production of four sets of round panel specimens using two fibre-reinforced concrete (FRC) mixtures and two FRS mixtures. The fibre type and content and the target compressive strength of each mixture are given in Table 1. Forty (40) panels were made from each mixture and were tested subsequently using four different servo-hydraulic testing machines located at TSE P/L and the University of Western Sydney (UWS), Australia. Table 2 indicates the testing machines and the measured load train stiffness (k). Ten replicate specimens from each mixture were tested using each machine.

Specimens were made from the FRC or FRS mixture by casting in moulds. Concrete was supplied from a dry-batch ready-mixed plant and delivered as a 3.0 m^3 batch in a 5.6 m^3 truck-mounted agitator. Fibres were added on top of the concrete and mixed in for 15 minutes at high-speed rotation. The round moulds were laid horizontally on the ground and concrete with fibres mixed in was dispensed via the chute directly into the moulds. The concrete was vibrated using an internal vibrator, then screeded and floated using the procedure described in the Appendix of ASTM C1550.

After finishing, the specimens were covered with plastic sheeting and allowed to harden for two days before stripping and transfer to tanks containing lime-saturated water. Immersion curing in water continued for 3–5 months after which the specimens were withdrawn and tested in a surface-moist condition. The 10 specimens tested using each of the machines listed in Table 2 were randomly selected from the 40 produced as part of each casting trial.

Table 1. Mixtures used in first ILS.

Set	Fibre	Description
A1	9 kg/m^3 Strux 85/50	25 MPa cast FRS
A2	60 kg/m^3 Wavecut 25 × 0.7 mm	25 MPa cast FRC
A3	30 kg/m^3 Novotex 0730	32 MPa cast FRC
A4	8 kg/m^3 Kyodo 48 mm	32 MPa cast FRS

Table 2. Testing machines used in first ILS.

Rig	Facility	Machine	k (N/mm)
1	UWS	3000 kN Instron 8506	72300
2	UWS	1000 kN Instron 8800	72400
3	TSE	100 kN MTS 244.21	51300
4	TSE	250 kN MTS 244.31	53100

Because the first ILS involved only four testing machines from two facilities located in Sydney, the results were regarded as unlikely to satisfy the requirements for a general estimation of multi-laboratory precision of ASTM C1550. A second larger study was therefore undertaken with support from the ASTM ILS program.

The second inter-laboratory study involved six sets of round panel specimens using three FRC mixtures and three FRS mixtures. The fibre type and content and the target compressive strength of each mixture are given in Table 3. Thirty-six (36) panels were made from each mixture and were tested subsequently using six different servo-hydraulic testing machines located at five facilities (TSE P/L; UWS, BASF in Cleveland, Ohio; University of Greenwich, Kent, U.K.; and University of Luleå, Sweden). Table 4 indicates the testing machines and the measured load train stiffness (k). The results from each machine at UWS were treated as coming from a different "laboratory". Six replicate specimens from each mixture were tested using each machine.

Production of the specimens was achieved either by casting or spraying. Concrete was supplied from a dry-batch ready-mixed plant and delivered

Table 3. Mixtures used in second ILS.

Set	Fibre	Description
B1	6.4 kg/m^3 Kyodo 48 mm	40 MPa FRS
B2	8 kg/m^3 Enduro 50 mm	32 MPa FRS
B3	40 kg/m^3 Dramix RC 65/35	32 MPa FRS
B4	37.5 kg/m^3 Novotex 0730	20 MPa cast FRC
B5	5 kg/m^3 Shogun 48 mm	20 MPa cast FRC
B6	25 kg/m^3 Novotex 1050	25 MPa cast FRC

Table 4. Testing machines used in second ILS.

Facility	Machine	k (N/mm)
UWS	3000 kN Instron 8506	72300
UWS	1000 kN Instron 8804	72400
TSE	250 kN MTS 244.31	53100
BASF	1300 kN Instron 300	–
Greenwich	DARTEC 500 kN	120900
Luleå	Eland 1000 kN	157000

as a 3.0 m^3 batch in a 5.6 m^3 truck-mounted agitator. Fibres were added on top of the concrete and mixed in for 15 minutes on high speed rotation. For the cast specimens, round moulds were laid horizontally on the ground and concrete with fibres mixed in was dispensed via the chute directly into the moulds. The concrete was vibrated using an internal vibrator, then screeded and floated. The sprayed specimens were produced by placing the moulds against a rack at approximately 45° to the horizontal and manually spraying shotcrete into the forms starting at the bottom and moving upward. Set accelerator was used at a dosage rate of approximately 5% by mass of cement. The inclined specimens were screeded and floated in the inclined position before being lowered to the horizontal position and finished with a steel float.

After finishing all specimens were covered with plastic sheeting and allowed to harden for two days before stripping and transfer to tanks containing lime-saturated water. Immersion curing in water continued for 6 months after which the specimens were stored in an external shaded but dry environment for 18 months. They were then placed in crates for shipping to the various facilities. All specimens were tested within a period of approximately 4 weeks and at an age of approximately two and a half years. The specimens to be tested at each facility were selected successively from the 36 panels produced for each mixture. Thus, every sixth panel was tested on the same machine (e.g., panels 1, 7, 13, etc.). This ensured that the six specimens from each mixture to be tested on the same machine represented material from throughout the entire load of concrete used to make the specimens.

2.2 *Data analysis*

In both inter-laboratory studies the measured parameters included peak load and energy absorption sustained at 5, 10, 20, and 40 mm central deflection. The Appendix provides test results from the first ILS and the results from the second ILS are available in Bernard & Carino (2009).

ASTM C1550 requires the formation of at least three radial cracks in a panel specimen for a valid test. In each ILS, some specimens did not meet this requirement, so some test results had to be discarded. Therefore, the data sets were not "balanced", that is, they did not have the same number of replicate test results for each combination of laboratory and mixture (or "cell"). This affected the data analysis methods that were used.

The objective of the data analysis in an ILS programme is to determine the single-operator index of precision (standard deviation or coefficient of variation [COV]) and the multi-laboratory index of precision. The former is usually called "repeatability" and the latter is usually called "reproducibility". For balanced data sets, that is, equal number of replicates in each cell, procedures for calculating these quantities can be found in ASTM C802 or ASTM E691.

In the first ILS, only one specimen failed to meet the three radial-cracks requirement of ASTM C1550. The single-operator variance (standard deviation squared) for each mixture was obtained by pooling the variances from the four testing machines. The between laboratory component of variance (s_b^2) for each mixture was obtained by using analysis of variance (ANOVA) with a correction factor for unequal data sets (Mandel & Paule 1970; Montgomery 1984). The following equation was used:

$$s_b^2 = \frac{(p-1)MS_b - MS_w}{\sum n_i - \frac{\sum n_i^2}{\sum n_i}} \tag{1}$$

In Eqn. (1), MS_w is the within-laboratory mean square and MS_b is the between-laboratory mean square obtained from the ANOVA table. The number of laboratories is p and the number of replicates for each laboratory is n_i.

In the second ILS, 11 specimens had less than three radial cracks: mixture 4 had two cases; mixture 5 had three cases; and mixture 6 had six cases. Although the between-laboratory component of variance can be estimated using Eqn. (1), the method described by Mandel & Paule (1970, 1982) was instead used. Mandel & Paule argue that the analysis of variance approach gives equal weighting to each result, and a better approach is to use a weighting based on the inverse of the variance associated with each cell (particular combination of laboratory and mixture).

Basically, the Mandel-Paule method uses an iterative procedure to obtain an estimate of the between-laboratory component of variance (s_b^2) and of the weighted grand mean for each test parameter (peak load and energy absorption). The steps used to estimate the between-laboratory component of variance and the grand mean for each parameter in the second ILS are presented in Bernard & Carino (2009).

In general, the between-laboratory component of variance is defined as follows:

$$s_b^2 = s_{\bar{Y}}^2 - \frac{s_w^2}{n} \tag{2}$$

In Eq. (2), $s_{\bar{Y}}^2$ is the variance of the laboratory averages for a particular mixture, s_w^2 is the pooled single-operator variance, and n is the number of replicates. Where there is a small variation among the laboratory averages, Eqn. (2) may result in a

negative value for s_b^2. In such cases, ASTM C802 and ASTM E691 state that s_b^2 is to be assigned a value of zero.

ASTM C1550 defines a test result as the average of at least two individual determinations. For the case where two replicate determinations comprise a test result, the multi-laboratory variance (s_R^2) is computed as follows:

$$s_R^2 = s_b^2 + \frac{s_w^2}{2} \quad (3)$$

The multi-laboratory variance for individual determinations would be obtained by replacing the number 2 in Eq. (3) with the number 1.

2.3 *Results of data analysis*

2.3.1 *Single-operator precision*

The values of the pooled single-operator standard deviations s_w for peak load are shown as a function of the average peak load for each mixture in Figure 2.

Several observations are noted. First, the range of the average peak loads is limited. Second, the standard deviations from the first ILS appear to have a linear dependence on average load, which implies that the coefficient of variation may be used as the measure of variability. Third, for the second ILS, the standard deviation did not appear to depend on the peak load. The last observation implies that the standard deviation is constant, which is not typical of concrete strength tests. It was found that if straight lines are fitted through the origin for each data set, the slopes are the same with a value of 0.062. Thus it may be concluded that the single-operator coefficient of variation for peak load is 6.2% with a 95% confidence interval of 5.2% to 7.2%.

The single-operator standard deviation for the energy absorption parameters is shown as a function of the average value in Figure 3. There are three significant observations. First, the standard deviation appears to increase linearly with average energy absorption. Second, the results for the two ILS programs appear to be similar. Third, the results for the different energy parameters appear to fall along a common line.

The first observation supports the use of coefficient of variation as the measure of single-operator variability. To examine whether the results for each energy parameter from the two ILS programs can be combined, the confidence intervals for the slopes of the best-fit straight lines through the origin for each ILS were compared. Columns 4 and 5 in Table 5 show the 95% confidence limits

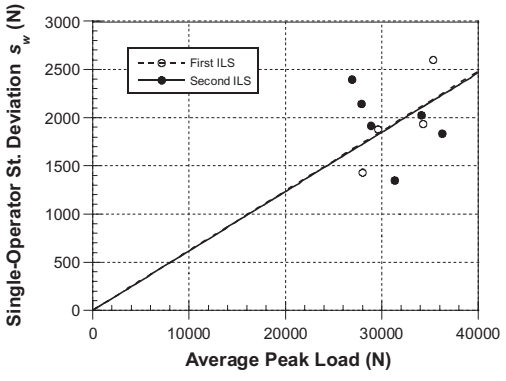

Figure 2. Single-operator standard deviation for peak load as a function of average peak load for each mixture.

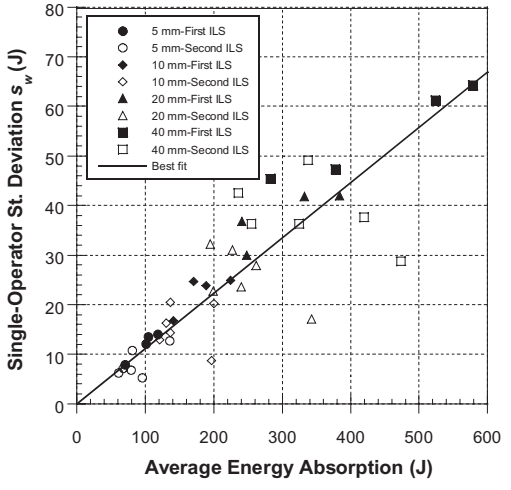

Figure 3. Single-operator standard deviation for energy absorption as a function of average energy absorption for each mixture.

Table 5. Single-operator coefficient of variation COV_w for energy absorption parameters.

Energy	ILS	COV_w	Lower 95%	Upper 95%	Combine	COV_w
T-5	1	12.1%	11.0%	13.2%	Yes	10.5%
	2	9.2%	6.6%	11.9%		
T-10	1	12.3%	10.0%	14.7%	Yes	10.9%
	2	9.7%	5.7%	13.6%		
T-20	1	12.3%	9.6%	14.9%	Yes	11.1%
	2	9.8%	5.5%	14.2%		
T-40	1	12.0%	9.4%	14.6%	Yes	11.3%
	2	10.4%	6.0%	14.8%		

for the best-fit slopes expressed in percent (these represent the single-operator coefficients of variation). If the confidence intervals of the coefficients of variation for each energy parameter overlap, the two sets of ILS data can be combined. The column labeled "Combine" indicates whether the confidence intervals of COV_w overlap. It is seen that for each energy parameter, the data from the two ILS programs can be combined. The last column of Table 5 shows the resulting best-fit value of COV for each energy parameter. These values are remarkably similar, and it is reasonable to compute a single best-fit slope for the combined data in Fig. 3. The computed slope for a line through the origin is 0.111 with a 95% confidence interval of 0.101 to 0.121. Thus, for the energy absorption parameters, the single-operator COV for the ASTM C1550 test is approximately 11%.

2.3.2 *Multi-laboratory precision*

The multi-laboratory standard deviation s_R was calculated by taking the square root of the variance computed in accordance with Eq. (3). Figure 4 shows the resulting values of s_R for peak load for the two ILSs. There are two notable observations: firstly, the standard deviation appears to increase with average peak load; and secondly, the linear trends do not appear to be the same for the two studies. Thus it can be concluded that COV is an appropriate measure of multi-laboratory precision. For the first ILS, the best-fit value for multi-laboratory coefficient of variation (COV_R) is 5.3% with a 95% confidence interval of 4.1% to 6.5%. While for the second ILS, the best-fit value is 8.9% with a 95% confidence interval of 7.4% to 10.3%. Because the confidence intervals do not overlap, the COV_R values are different for these two studies. Thus an upper estimate of multi-laboratory COV for peak load of the ASTM C1550 test is about 9%.

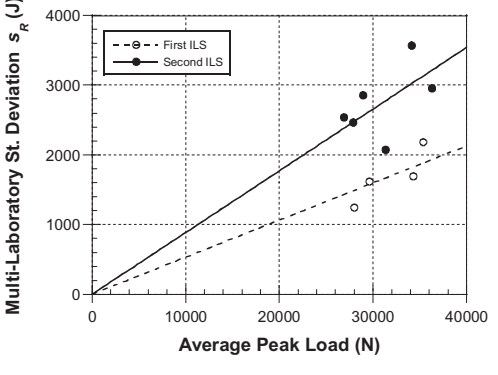

Figure 4. Multi-laboratory standard deviation for peak load as a function of average peak load for each mixture.

The multi-laboratory standard deviation for the energy absorption parameters is shown as a function of the average value in Figure 5. It is clear that the standard deviation increases with the average value of energy absorbed. The same approach as used for the single-operator results was used to examine whether the multi-laboratory results from the two studies can be combined, and whether the results for the different energy parameters can be combined.

Table 6 shows the 95% confidence intervals for the best-fit values of COV_R for the various energy absorption parameters from the two ILS programs. The overlapping confidence intervals for each parameter indicate that the results from the two ILSs can be combined. The resulting best-fit values for COV_R for each energy parameter using the combined data are shown in the last column of

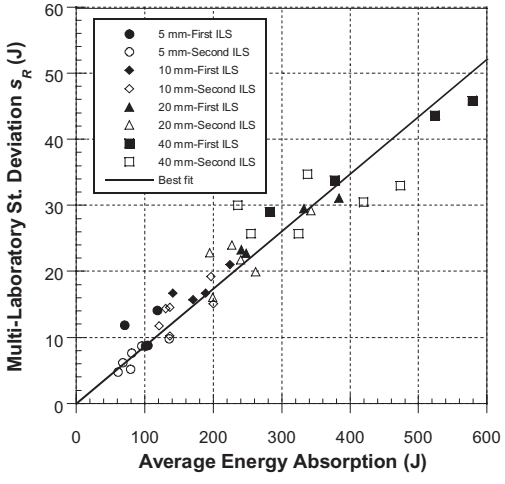

Figure 5. Multi-laboratory standard deviation for energy absorption as a function of average energy absorption for each mixture.

Table 6. Multi-laboratory coefficient of variation COV_R for energy absorption parameters.

Energy	ILS	COV_R	Lower 95%	Upper 95%	Combine	COV_R
T-5	1	10.8%	5.7%	15.9%	Yes	9.3%
	2	8.0%	6.8%	9.3%		
T-10	1	9.6%	7.8%	11.4%	Yes	9.3%
	2	9.1%	7.6%	10.7%		
T-20	1	8.7%	7.7%	9.8%	Yes	8.9%
	2	9.0%	7.6%	10.4%		
T-40	1	8.5%	7.2%	9.7%	Yes	8.4%
	2	8.4%	6.3%	10.4%		

Table 6. The COV_R values for each energy parameter are similar to each other, and it is appropriate to combine all the data and compute a single value. When this is done, the best-fit value of COV_R for the energy absorption parameters is 8.7% with a 95% confidence interval of 8.3% to 9.1%. Thus for the energy absorption parameters, the multi-laboratory COV for the ASTM C1550 test is approximately 8.7%. Keep in mind that this is based on comparing the averages of the results of *two* individual test specimens (Eqn. (3)).

2.4 *Summary*

The data from two ILS programs of ASTM Test Method C1550 have been analyzed to provide information on the inherent precision of the method. The first ILS involved four materials, four testing machines and 10 replicates. The second ILS involved six materials, six testing machines, and six replicates.

Because some of the individual test results had to be discarded, the methods in ASTM C802 and ASTM E691 for evaluating the between-laboratory component of variance were not applicable. For the first ILS, only one test result for each performance parameter had to be discarded (see the Appendix for all results obtained in the first ILS). In this case, analysis of variance was used to compute the between-laboratory component of variance. For the second ILS, 11 tests results had to be discarded, and the method of Mandel & Paule (1970, 1982) was used. An ASTM Research Report giving the details of the data analysis of the second ILS is available (Bernard & Carino 2009).

ASTM C1550 requires that a test result includes at least two individual determinations. Therefore, the multi-laboratory variance s_R^2 was computed for a test result defined as the average of two individual determinations (Eq. (3)).

The analysis showed that, in general, the single-operator and multi-laboratory standard deviations increased with the average value of the property. Therefore, the COV was used as the measure of precision. Linear regression for lines passing through the origin was used to obtain the best-fit estimates for the single-operator and multi-laboratory coefficients of variation. The 95% confidence intervals for the estimates were used to assess whether the results from the two ILS programmes could be combined. For the energy absorption parameters, it was found that the level of deflection did not have a significant effect on the variability of measured energy absorption.

Analysis of the data obtained from the two ILS programmes is summarized in Table 7. For the multi-laboratory COV for the peak load the two ILS programs gave different values. The COV_w of 9% is the higher value obtained from the second ILS and is an upper estimate. In accordance with ASTM C670 or ASTM E177, the maximum difference (as percent of their average) between two test results that is expected in 95 out of 100 cases is obtained my multiplying these coefficients of variation by 2.8. Again, for the multi-laboratory case, a "result" is the average of *two* individual determinations.

Table 7. Single-operator and multi-laboratory coefficients of variation for ASTM C1550.

Performance parameter	Single-operator, COV_w	Multi-laboratory, COV_R
Peak load	6.2%	≈9%
Energy absorption	11%	8.7%

3 VARIANCE IN FIELD-PRODUCED DATA

The ILS data presented above were derived from specimens produced under laboratory conditions. The objective of the second study presented in this paper was to assess the within-batch variability of performance parameters obtained using ASTM C1550 panels made in the field. This study also examined the characteristic distribution of individual results within a set of QC specimens and the distribution of within-batch COV data.

3.1 *Distribution of within-batch results*

Over the last 10 years the ASTM C1550 panel test has been used for QC purposes on numerous tunneling projects and in most underground metalliferous mines in Australia. The 100 kN MTS testing machine operated by TSE P/L has been used to conduct at least 6,000 ASTM C1550 tests on specimens produced in the field over this period. Several projects have involved in excess of 1000 panels, usually produced in sets of 2 or 3. The individual specimen results within each set of QC results were normalized with respect to the mean for each corresponding set and plotted as a histogram in Figure 6. This data therefore represents the distribution of the relative magnitude of individual test results within each batch with respect to the arithmetic mean for that batch.

The frequency distribution shown in Figure 6 shows that a modified Gaussian curve fitted to the field data using singular value decomposition (Johnson et al. 1994) produced an exceptionally good fit with $r^2 = 0.9960$. This function is plotted as the solid line in Figure 6. The expression for the Modified Gaussian curve is

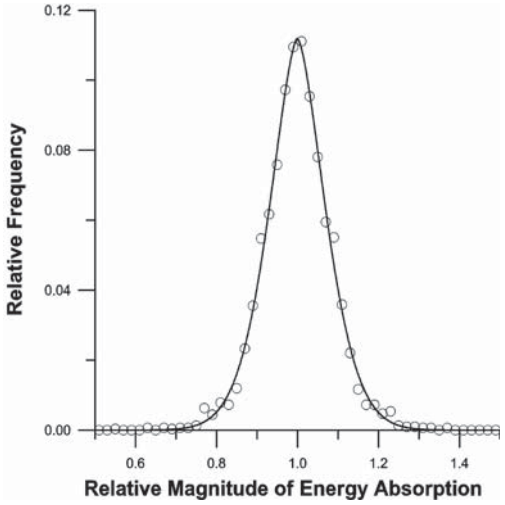

Figure 6. Distribution of the magnitude of energy absorption data at 40 mm relative to the within-batch mean for the corresponding batch (circles) for 3250 ASTM C1550 panels produced as part of QC programmes in Australian mines and tunnels.

$$y = a\exp\left[-\frac{1}{2}\left(\frac{|x-b|}{c}\right)^{d}\right] \tag{4}$$

in which $a = 0.111909$, $b = 0.99985$, $c = 0.064243075$, and $d = 1.602313$. When the conventional Gaussian curve is used (for which $d = 2$), $r^2 = 0.993$. These results indicate that individual energy absorption data from field-produced specimens are normally distributed about the arithmetic mean.

3.2 *Within-batch COV*

The within-batch COV was calculated for energy absorption at 40 mm central deflection for all pairs of field-produced specimens available and has been presented as a frequency distribution in Figure 7. The distribution shows that the within-batch COV is asymmetrically distributed with a long tail in the distribution toward larger values. This shows that for a sample size of two there is large variability in the calculated coefficient of variation (or standard deviation).

The overall shape of the frequency distribution defined by the points in Figure 7 is similar to Helmert's equation (Deming, 1950) for the sampling distribution function of the sample standard deviation computed from two replicate specimens taken from a normal distribution. Thus the data were fitted with a function analogous to Helmert's

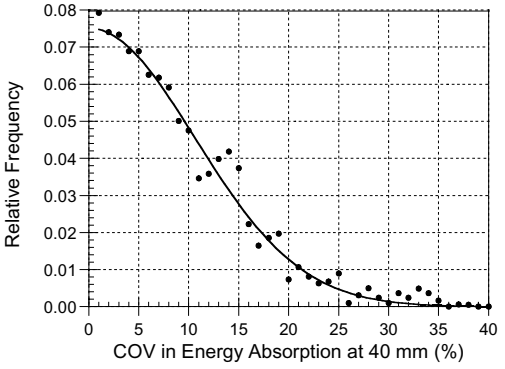

Figure 7. Distribution of within-batch coefficients of variation (COV) in energy absorption at 40 mm for replicate specimens ($n = 2$) produced in selected mining and tunneling projects within Australia.

distribution with the COV substituted for the standard deviation.

For the case where standard deviation is based on $(n - 1)$ degrees of freedom, Helmert's distribution function for the standard deviation is given by the following:

$$f(s) = 2\frac{\left(\frac{n-1}{2\sigma^2}\right)^{(n-1)/2}}{\Gamma((n-1)/2)} s^{n-2}\, e^{-(n-1)\,s^2/(2\sigma^2)} \tag{5}$$

in which Γ is the gamma function. In Eqn. (5), σ is the population standard deviation and s is the computed value of standard deviation based on n replicate tests. For the case $n = 2$, $\Gamma(0.5) = 1.7725$. If s is replaced with V (for coefficient of variation), the distribution function for the coefficient of variation based on two replicates is as follows

$$f(V) = \frac{0.7979}{V_{\text{inf}}} e^{-0.5V^2/V_{\text{inf}}^2} \tag{6}$$

The only adjustable parameter in Eq. (6) is the value of V_{inf}, which is the true coefficient of variation for the population. Figure 7 shows the resulting best-fit curve to the data, and the estimated value of V_{inf} is 10.6%.

The average within-batch COV for the data of energy absorption at 40 mm central deflection obtained from field-produced panels is about 9% (a similar level was obtained for energy absorbed at 5, 10, and 20 mm central deflection). However from the fitted distribution function, the within-batch COV for the population is estimated to be 10.6%. This difference may be attributed to the effect of the number of replicates on the computed COV, as discussed in the authors' companion paper in

these proceedings (Bernard et al., 2010). The COV obtained using two replicate specimens will underestimate the true COV for the population. From the two ILS programmes, the within-batch COV for energy absorption parameters was estimated to be 11%. This compares favorably with the estimate based on field results.

ACKNOWLEDGEMENTS

The authors wish to thank the following for their contribution to this work: ASTM International for financial assistance in conducting the ILS studies; BASF, the University of Western Sydney, the University of Greenwich, and the University of Luleå for participation in the ILS; BHPB Cannington and BHBP Olympic Dam for permission to use QC data, and EPC P/L for assistance in conducting the PDP study.

REFERENCES

American Concrete Institute 506.1R, 2008. *Guide to Fiber-Reinforced Shotcrete*, ACI, Farmington Hills.

ASTM International, 2008. Practice C670, "Standard Practice for Preparing Precision and Bias Statements for Test Methods for Construction Materials,"

ASTM International, 2008. Practice C802, "Standard Practice for Conducting an Interlaboratory Test Program to Determine the Precision of Test Methods for Construction Materials," ASTM, West Conshohocken, Pa.

ASTM International, 2008. Test Method C1550, "Standard Test Method for Flexural Toughness of Fiber Reinforced Concrete (Using Centrally Loaded Round Panel)," ASTM, West Conshohocken, Pa.

ASTM International, 2008. Practice E177, "Standard Practice for Use of the Terms Precision and Bias in ASTM Test Methods," ASTM, West Conshohocken, Pa.

ASTM International, 2008. Practice E691, "Standard Practice for Conducting an Interlaboratory Study to Determine the Precision of a Test Method," ASTM, West Conshohocken, Pa.

Bernard, E.S., 2000. "Behaviour of round steel fibre reinforced concrete panels under point loads", *Materials and Structures*, RILEM, Vol. 33, April, pp. 181–188.

Bernard, E.S. 2002. "Correlations in the behavior of fiber reinforced shotcrete beam and panel specimens", *Materials and Structures*, RILEM, Vol. 35, April, pp. 156–164.

Bernard, E.S., 2005. "The Role of Friction in Post-crack Energy Absorption of Fiber Reinforced Concrete in the Round Panel Test", *Journal of ASTM International*, January, Vol. 2, No.1, pp. 1–12.

Bernard, E.S. and Pircher, M., 2001. "The Influence of Thickness on Performance of Fiber-Reinforced Concrete in a Round Determinate Panel Test", *Cement, Concrete, and Aggregates*, CCAGDP, Vol. 23 No. 1, pp. 27–33.

Bernard and Carino, N., 2009, "Interlaboratory Study to Establish Precision Statements for ASTM C1550, Standard Test Method for Flexural Toughness of Fiber Reinforced Concrete (Using Centrally Loaded Round Panel)", ASTM Report RR-XXXX, ASTM International, www.astm.org.

Bernard, E.S., Xu., G.G. and Carino, N.J., 2010. "Influence of the number of specimens in a batch on apparent variability in FRS performance assessed using ASTM C1550 panels," *Shotcrete: Elements of a System*, Taylor & Francis, London.

CIA, 2008. *Shotcreting in Australia: Recommended Practice*, Concrete Institute of Australia & AuSS, Sydney.

Deming, W.E., 1950. *Some Theory of Sampling*, Wiley.

EFNARC, 1996. *European Specification for Sprayed Concrete*, European Federation of National Associations of Specialist Contractors and Material Suppliers for the Construction Industry.

EN 14488 *Testing Sprayed Concrete*, European Standards (Euronorm), European Committee for Standardisation.

Hanke, S.A., Collis, A. and Bernard, E.S. 2001. "The M5 motorway tunnel: an education in Quality Assurance for fiber reinforced shotcrete", *Shotcrete: Engineering Developments*, Bernard (ed.), 145–156, Swets & Zeitlinger, Lisse.

Johnson, N. L., Kotz, S. and Balakrishnan, N. 1994. *Continuous Univariate Distributions* Vol. 1, 2nd Ed., John Wiley & Sons, New York.

Kendall, M. and Stuart, A. 1979. *The Advanced Theory of Statistics, Volume 2: Inference and Relationship*, 4th Ed., Charles Griffin & Co., England.

Law, A.M. and Kelton, W.D., 2000. *Simulation Modelling and Analysis*, 3rd Ed., McGraw-Hill New York.

Mandel, J. and Paule, R. C., 1970. "Interlaboratory Evaluation of a Material with Unequal Number of Replicates", *Analytical Chemistry*, Vol. 42, No, 11, pp. 1194–1197.

Montgomery, D.C., 1984. *Design and Analysis of Experiments*, John Wiley & Sons Inc.

Paule, R.C. and Mandel, J., 1982. "Consensus Values and Weighting Factors", *Journal of Research of the National Bureau of Standards*, Vol. 87, No. 5, pp. 377–385.

Roux, J., Cheminais, J., Rivallain, G. and Mourand, C., 1989. 'Béton projeté par voie sèche avec incorporation de fibres', *Tunnels et Ouvrages Souterrains*, 92 pp. 61–97.

APPENDIX

This appendix contains summarized results for all four sets of specimens produced and tested as part of the first ILS reported in the main text of this paper.

Table A1. Test results from first ILS, Specimen Set 1.

Machine	Peak load (N)	Energy absorption 5 mm (J)	10 mm (J)	20 mm (J)	40 mm (J)
Instron 8506 3000 kN	31791	103	196	355	574
	31159	112	208	367	582
	31174	129	252	451	717
	30159	95	174	298	470
	32157	113	210	368	573
	33050	112	203	350	547
	29998	99	185	324	501
	28578	95	178	316	505
	27280	79	147	260	418
	31120	120	230	406	641
Instron 8800 1000 kN	26471	76	143	255	416
	30733	110	206	362	539
	27597	99	185	322	508
	31218	97	177	310	498
	31064	114	214	373	588
	30242	96	179	312	496
	29736	93	173	301	476
	27531	99	188	340	554
	31153	95	176	308	481
	33027	125	231	396	582
MTS 243 100 kN	28087	90	169	302	490
	33104	122	229	400	625
	31729	127	240	416	607
	28853	85	158	279	444
	27049	92	175	310	502
	29597	99	182	316	499
	31357	100	183	323	516
	31843	102	183	309	454
	29637	106	197	343	543
	26888	98	184	328	528
MTS 244 250 kN	27025	87	165	291	472
	28101	95	183	323	519
	27858	101	194	347	543
	27031	95	181	320	516
	28694	91	173	304	480
	27307	101	192	336	538
	32035	103	191	344	565
	27375	94	179	321	511
	26707	90	163	280	442
	28341	98	183	315	489

Table A2. Test results from first ILS, Specimen Set 2.

Machine	Peak load (N)	Energy absorption 5 mm (J)	10 mm (J)	20 mm (J)	40 mm (J)
Instron 8506 3000 kN	37036	119	189	243	244
	38949	113	182	253	292
	37947	112	184	261	305
	39415	128	214	303	347
	25170	89	144	201	237
	36977	111	178	250	296
	33456	98	162	233	278
	33805	96	158	229	276
	37335	109	183	255	299
	35472	81	126	174	205
Instron 8800 1000 kN	35281	99	163	233	276
	37053	108	175	249	294
	39279	121	199	291	362
	35281	109	181	267	332
	37458	120	201	290	342
	32737	78	125	173	202
	38761	112	187	271	318
	35077	87	137	197	238
	35746	105	165	230	268
	35268	93	145	203	240
MTS 243 100 kN	33244	88	140	194	224
	39011	119	190	259	290
	34754	110	173	234	263
	37222	97	159	226	269
	37670	111	181	257	306
	39963	101	158	224	266
	35787	110	174	243	284
	34190	111	184	265	314
	36970	124	207	299	361
	35084	94	148	205	219
MTS 244 250 kN	33036	108	186	271	320
	32464	104	174	245	278
	32583	109	178	252	299
	35414	131	223	324	383
	33674	95	157	223	266
	32267	89	142	201	241
	33139	113	189	270	324
	32416	91	147	210	242
	35186	99	164	233	272
	32605	80	132	189	233

Table A3. Test results from first ILS, Specimen Set 3.

Machine	Peak load (N)	Energy absorption 5 mm (J)	10 mm (J)	20 mm (J)	40 mm (J)
Instron 8506 3000 kN	30513	100	184	311	473
	32286	119	221	374	550
	35177	123	228	390	590
	36038	141	255	423	636
	38282	144	270	460	701
	37321	156	287	481	717
	36041	121	227	391	590
	33437	121	234	394	590
	33856	136	250	414	617
Instron 8800 1000 kN	33252	108	201	311	442
	36294	121	219	362	530
	31850	100	181	306	465
	34153	120	228	397	617
	36056	139	263	445	673
	34519	121	227	395	605
	38351	138	254	434	643
	32821	149	269	444	655
	33377	127	236	416	635
	34886	128	235	394	588
MTS 243 100 kN	33016	98	191	331	504
	34231	104	194	327	479
	33760	100	198	349	526
	39245	145	269	435	604
	33751	104	203	351	532
	37592	127	247	422	635
	34283	114	213	364	545
	36647	128	248	426	640
	36112	123	238	415	635
	34395	102	199	341	498
MTS 244 250 kN	33195	104	210	376	579
	32620	109	208	363	548
	32768	107	212	372	576
	34544	107	204	355	534
	34090	114	222	391	604
	33193	101	214	381	587
	32042	99	200	364	578
	31315	105	202	355	545
	31708	110	217	378	578
	30991	89	184	330	509

Table A4. Test results from first ILS, Specimen Set 4.

Machine	Peak load (N)	Energy absorption 5 mm (J)	10 mm (J)	20 mm (J)	40 mm (J)
Instron 8506 3000 kN	26624	68	132	228	353
	28214	73	144	254	394
	24408	89	161	250	325
	27848	82	162	277	429
	26902	74	136	226	334
	29551	73	141	241	359
	25380	67	129	223	345
	27031	77	146	244	372
	27943	80	158	270	408
	28426	77	149	256	381
Instron 8800 1000 kN	27866	94	176	292	415
	30646	76	141	237	356
	27860	75	149	266	414
	28186	82	158	271	414
	30030	86	166	290	454
	30102	81	158	278	432
	31719	92	165	257	351
	27448	63	120	206	317
	27577	86	163	275	415
	29808	84	165	287	443
MTS 243 100 kN	26612	43	97	195	306
	27972	52	115	224	349
	28142	69	157	298	457
	29655	74	166	310	474
	28070	55	124	236	363
	29110	59	137	265	409
	29687	64	138	254	384
	28420	51	109	203	318
	30475	55	117	225	333
	25017	48	101	193	304
MTS 244 250 kN	27240	67	137	245	388
	28661	77	164	296	452
	26143	63	119	198	288
	27246	71	142	249	389
	26488	67	135	233	351
	29283	75	153	274	420
	27383	59	120	209	324
	26855	66	133	233	370
	28590	68	130	232	367
	27163	60	123	219	343